

We are IntechOpen, the world's leading publisher of Open Access books Built by scientists, for scientists

6,900

Open access books available

186,000

International authors and editors

200M

Downloads

Our authors are among the

154

Countries delivered to

TOP 1%

most cited scientists

12.2%

Contributors from top 500 universities



WEB OF SCIENCE™

Selection of our books indexed in the Book Citation Index
in Web of Science™ Core Collection (BKCI)

Interested in publishing with us?
Contact book.department@intechopen.com

Numbers displayed above are based on latest data collected.
For more information visit www.intechopen.com



Sol-Gel-Derived Doped ZnO Thin Films: Processing, Properties, and Applications

Asad Mahmood and Abdul Naeem

Additional information is available at the end of the chapter

<http://dx.doi.org/10.5772/67857>

Abstract

Sol-gel-derived zinc oxide (ZnO)-based materials with an improved microstructure are consumed in electronics and electrical frameworks owing to their crystal structure dependent properties, which can be exploited for optical, electrical, and photocatalytic applications. Despite research articles published each year on the strategies to improve the optoelectronic properties of ZnO, the topic is still actively pursued in literature. This chapter provides an insight into the recent developments for the sol-gel-derived processing of the pure and doped ZnO thin films. It also highlights the challenges and opportunities surrounding the processing of these devices. The recent developments in the synthesis of pure, doped ZnO, and corresponding applications of these films will be discussed in detail. Consequently, the aim of this chapter is to provide an overview of the novel developmental strategies to improve ZnO-based thin films by a sol-gel route with enhanced optical properties for practical applications ranging from optical and electrical circuits to sensing.

Keywords: sol-gel processing, zinc oxide, thin films, conductivity, optical properties.

1. Introduction

Zinc oxide, characterized as a direct wide band gap ($E_g \approx 3.37$ eV @ °T-Room) semiconductor, is a potential material for photonics and optoelectronic applications [1]. The large excitonic energy (60 mV), which renders an effectual excitonic emission in ZnO, is exploited for applications such as ultraviolet light-emitting and laser diodes. Moreover, the pure and doped ZnO has been investigated for applications in the solar cells, photoelectrochemical cells (PECs), thin film transistors, gas sensors and nanogenerators. ZnO can be used for all of these applications due to its chemical and physical stability, abundance, economical feasibility and

environment friendly. Also, due to its characteristic E_g and good optical transmittance, ZnO is well thought out in organic and solar hybrid cells, as a cathode buffer layer or, a transparent electrode. Crystalline ZnO exhibits superior electrical properties, both in the form of bulk and thin films. Due to factors such as small size, light weight, stability, and ability to configure in different frameworks, thin films are promising structures studied compared to their bulk counterparts. Undoped ZnO is seldom used, and the optoelectronic properties of ZnO are tailored for specific applications by various processing techniques, such as synthesis procedures, doping mechanism optimization, an introduction of impurities, controlling the microstructure, and the thickness of the films. Recent development in the nanoscience and nanotechnology has led to the miniaturization and diversification of the electronic and optical devices, which endeavor researchers to develop new synthetic strategies in order to process semiconductor-based thin films and powders on a viable scale [2].

ZnO films are useful for the transparent conductive layer applications in the LEDs, flat panel displays (FPD), and solar cells due to its high transmittance properties in the visible region and good electrical conductivity [3]. The electrical properties of ZnO are associated with the presence of interstitial Zn atoms and crystal defects, that is, oxygen vacancies due to the non-stoichiometry and defects generated in crystals during grain growth. To improve the conductivity in ZnO films compared to the metallic films, various elements in the form of impurities are introduced in the ZnO crystal lattice to replace Zn. The elements from group III (B, Al, Ga, and In) and group IV (Ti, Zr, Sn, and Hf) are commonly used to alter the properties of ZnO. The electronegativity and ionic radius are important parameters, which affect the dopant efficiency. Another approach is to modify the processing techniques to develop ZnO films with modified microstructure. The particle morphology such as from particles, tubes, and wires (in the nm or μm range), and film surface morphology influenced the properties of the aimed devices.

Zinc oxide exhibits a wurtzite hexagonal crystal structure ($a \approx 3.249 \text{ \AA}$; $c \approx 5.205 \text{ \AA}$ ICDD PDF no. 36-1451) [4]. The undoped ZnO structure is composed of alternating planes of tetrahedrally coordinated O^{2-} and Zn^{2+} ions along the c-axis (**Figure 1(a)**). The characteristic non-central symmetric structure and properties such as piezoactivity and pyroelectricity are associated with the tetrahedral coordination of ZnO. Further, ZnO exhibits polar surfaces, and the asel plane is the most common surface. The positively and negatively charged surfaces ($\text{Zn}_{-(0001)}$ and $\text{O}_{(0001)}$, respectively) are created due to the oppositely charged ions, which generate spontaneous polarization and normal dipole moment along the c-axis as well as a divergence in the surface energy. The lower valence band (VB) and the upper conduction band (CB) comprise the E_g of ZnO (**Figure 1(b)**). The given band structure for the pure ZnO was calculated using a VASP code [5]. At 0 K, the CB remains empty, while electrons only occupy the VB energy levels. Discrete energy levels are present in an isolated atom. However, the split in the energy level occurs during the crystal formation. In such a state, the closely spaced levels due to atomic interactions result in a continuous energy band. Various properties of the pure ZnO are presented in **Table 1**.

ZnO thin films are processed using methods such as atomic layer deposition (ALD) [7], chemical vapors deposition (CVD) [8], pulsed laser deposition (PLD) [9], RF magnetron sputtering

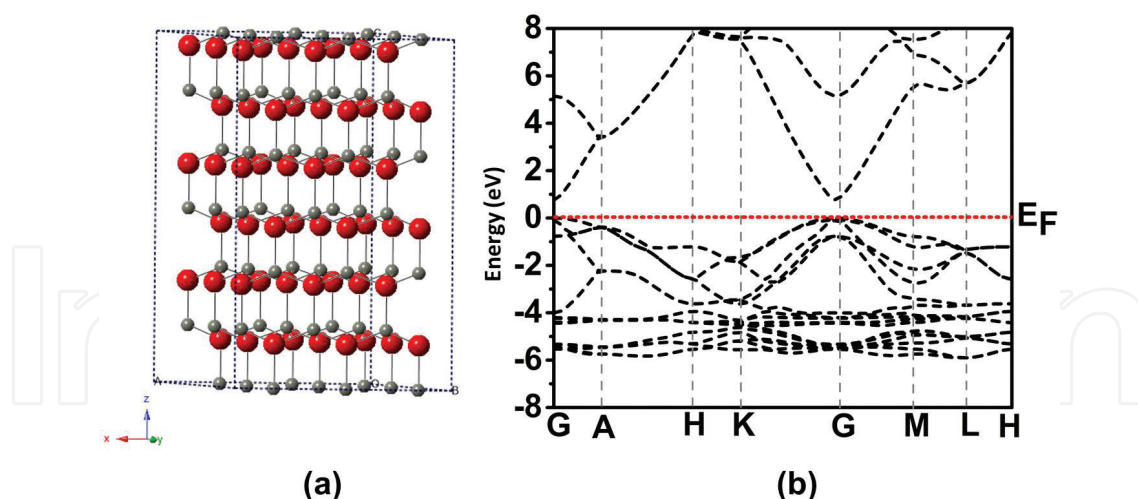


Figure 1. (a) Crystal structure ZnO. The small spheres represent zinc atoms, while the large spheres represent oxygen atoms; (b) calculated band structure of pure ZnO. The Fermi level (E_F) is set to 0 eV.

[10], epitaxial growth [11], self-assembly [12], sputtering technique [13], co-precipitation [14], electrodeposition [15], spray pyrolysis [16], and sol-gel method [17]. The sol-gel technique is also used for the fabrication of membranes [18], chemical sensors [19], optical gain media [20, 21], electrochemical devices [22], photochromic and non-linear applications [23], and nano-materials [24]. The sol-gel method is advantageous over other synthetic procedures. These advantages include as follows:

Properties	Characteristics
Crystal structure	Wurtzite
Lattice constant (a)	0.325 nm
Lattice constant (c)	0.521 nm
Density (kg/m^3)	5.6 gcm^{-3}
Exciton binding energy	60 mV
Static dielectric constant (ϵ_s)	7.9
Optical dielectric constant	3.7
Optical band gap energy (E_g)	3.2 eV
Flat band potential (E_{fb})	-0.5 V versus saturated calomel electrode (SCE)
Effective electron mass (M)	$0.24\text{--}0.3 m_e, m_e = 9.11 \times 10^{-31} \text{ kg}$
Effective hole mass (m_h)	$0.45\text{--}0.6 m_e, m_e = 9.11 \times 10^{-31} \text{ kg}$
Electron mobility (μ_e)	$200 \text{ cm}^2 \text{ V}^{-1} \text{ s}^{-1}$
Point of zero charge (Pzc)	8–9 pH

Table 1. Various properties of pure ZnO [6].

- The sol-gel product exhibits better homogeneity and purity.
- The sol-gel process can be conducted at low temperatures.
- The sol-gel process offers control over stoichiometry of multiphase systems, particle size, shape and physiochemical properties.
- The procedure can be used for thin film fabrication.
- Sol-gel can be used for the synthesis of various inorganic and organic hybrid materials.
- Sol-gel process is easier to control the microstructure during sintering (densification process).

These advantages allow for commercial processing compared to other techniques such as ALD, PLD, and magnetron sputtering, which are costly, inefficient for large production purposes and have lengthy processing times. While recent research provides novel approaches in the development of ZnO-based thin films, this chapter presents a review with a goal to help ensure the device fabrication based on the sol-gel-derived ZnO thin films with current understanding and future perspectives. This chapter provides a plan to improve the approaches to semiconductor material applications, made available to a wider community of academics and practitioners, and present techniques for optimizing the parameters for better device performance. The chapter concludes with a summary of the contribution of the doped ZnO-based materials as the potential candidate for gas sensing, photocatalytic, and thermoelectric applications. This chapter will also provide researchers currently working in the field a useful literature in the form of articles and reviews.

2. Processing

The sol-gel method was initially used in 1800s. Later, around 1900s, this technology was implemented by the Schott Glass Company (Jena, Germany). The record of publications in the literature (patents and journal articles) related to the processing of materials via the sol-gel route from 1980 to 2010 is given in **Figure 2**.

A schematic view of the sol-gel process for the development of ZnO-based films is given in **Figure 3**. The sol-gel method can be modified for different purposes, and the parameters discussed here are modified continuously. Generally, the first step in a sol-gel process is the selection of suitable precursors, which will react through various steps and finally converting to colloidal particles (sol) or polymeric gels. A stable sol is required for the thin film deposition, which can be deposited by spin coating, dip coating, or drop casting techniques, while the sol is converted to a polymeric gel in order to synthesize powders. Metal ions or other reactive elements surrounded by ligands are largely used as a precursor for the sol-gel reaction. The most important precursors utilized in this method are metal alkoxides $M(OR)_n$ and alkoxy silanes due to their radial reaction mode. Metal alkoxides are derivatives of alcohols, ROH, which are weak acids, economical (inexpensive) and results in high purity hydrated oxides [25, 26]. Alcohols, such as absolute ethanol and isopropanol, are used as solvents for alkoxides, because they are immiscible with water. In the case of ZnO, acetates (zinc acetate dihydrate; $Zn(CH_3COO)_2 \cdot (H_2O)_2$) are commonly used as the Zinc (Zn) precursor [27]. Other

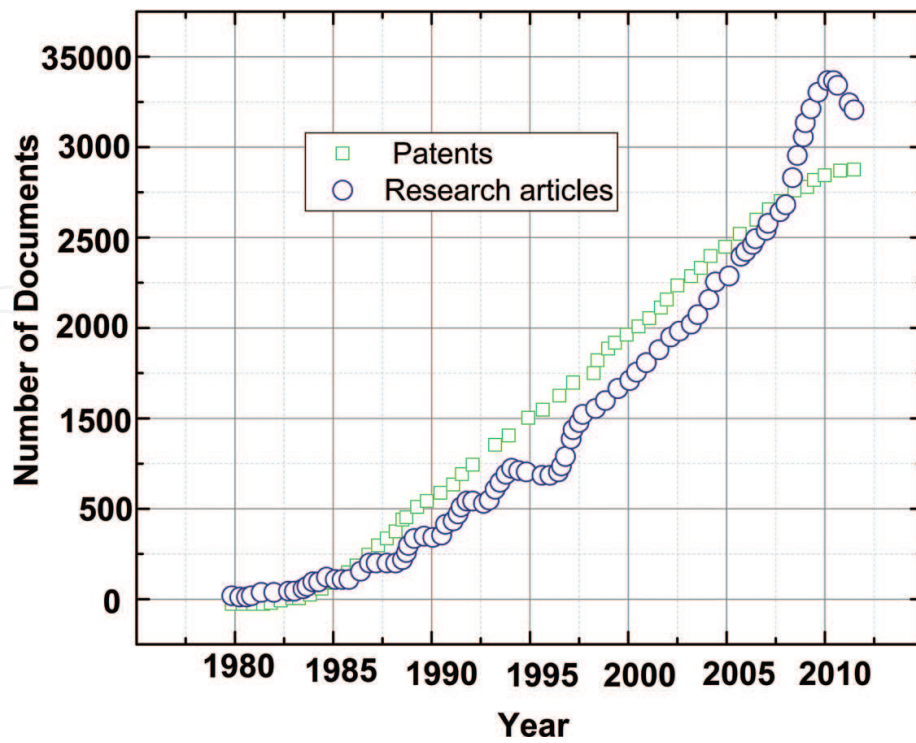


Figure 2. Publications in the sol-gel materials field, 1980–2010.

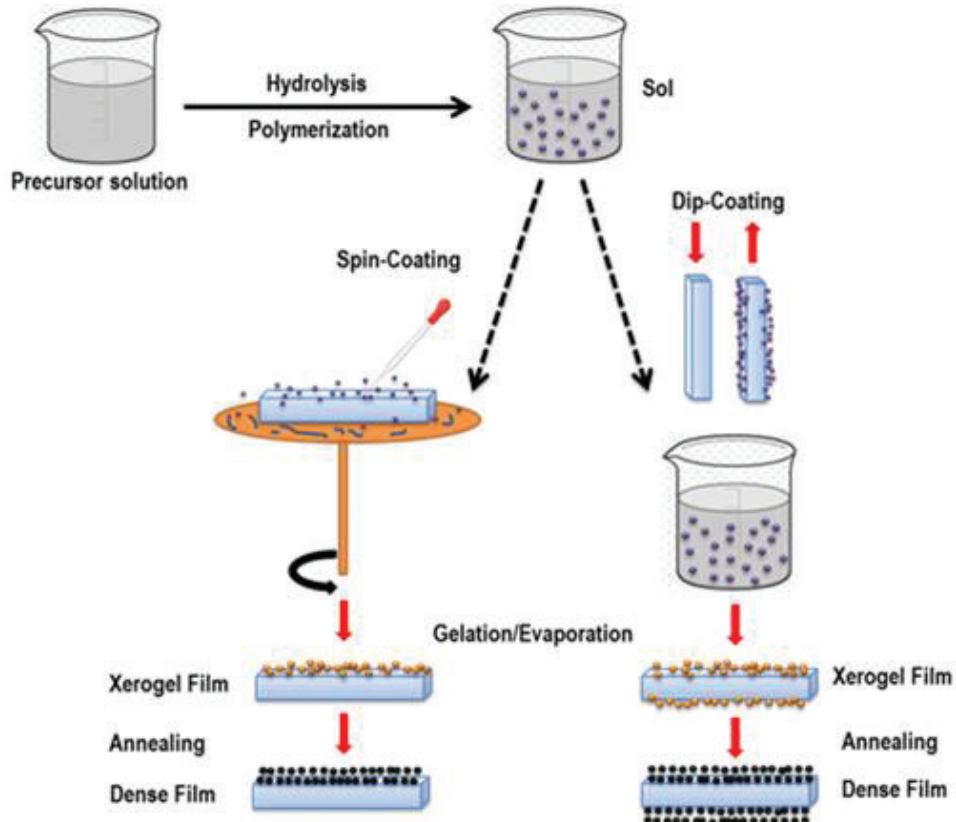


Figure 3. A schematic view of sol-gel process for the ZnO thin film processing.

Zn sources such as nitrate, acetylacetonate, perchlorate, and alkoxides (i.e., ethoxide, peroxides) are also used [28]. The alkoxide has disadvantages related to its high cost and sensitivity to moisture among others. On the contrary, metal salts are favored for large-scale production purposes. The Zn-salt plays an important role in developing a stable and clear colloidal solution. Acetates and nitrates are preferred compared to perchlorates, which might result in turbidity; however, the nitrate ions may result in the ionic impurities in the film annealing process. Further, the choice of precursor salt affects the morphology and hence the final properties of the films. The solvent used for the sol-gel process must exhibit a dielectric constant high enough to dissolve the metal salts. Generally, alcohols with low carbon number (i.e., methyl alcohol, ethyl alcohol, isopropanol, 1-butanol, and 2-methoxyethanol) are preferred as the potential solvents [29–32] and references therein. Ethylene glycol (boiling point; b.pt = 194.4°C) has also been reported exhibiting a dielectric constant of 40.61 (at 25°C) [33, 34].

During the sol-gel process, the precursor materials, that is, Zn source and the dopant elements (if applicable) in the predetermined stoichiometric ratios are first dissolved in a suitable solvent. In the second step, a stabilizing agent is added to the initial solution for the precursor metal(s). Monoethanolamine is a common stabilizer, which is used for the stabilization of Zn solution in sol-gel process. Acetylacetone, diethanolamine, tetramethylammonium hydroxide, and ethylenediamine tetraacetates are also used as stabilizers [27, 35]. A stabilizing agent is critical in sol-gel reactions to avoid both the premature precipitations and inhibiting the rapid conversion of the sol into a gel. In some cases, a catalyst is concurrently used for catalyzing the hydrolysis and condensation reactions. Some of the most common catalysts employed in sol-gel reactions are hydrochloric acid, potassium hydroxide, sodium hydroxide and ammonia [36]. The precursor solution is kept bathing on the magnetic hot plate with continued stirring until a clear and stable sol is achieved. The temperature is maintained (25–80°C) in an oil bath for homogeneous heating. The initial concentrations of the precursor materials, solvent to precursor ratios, and ratio of the stabilizing agents to the precursor are important as it can affect the solubility of precursors and stability of the sol. Furthermore, the concentration of the sol is an important factor, which defines the microstructure and thickness of films. Once a stable sol is achieved, it is aged for 24 h approximately at room temperature to confirm its stability. The stability is also checked by the Tyndall effect; laser light is applied to the solution, and the scattering phenomenon is investigated that is directly associated with the presence of small particles in the sol. The stable sols can be applied to different kinds of substrates using a drop casting, dip coating, and spin coating techniques. The speed of the spinning (revolution per minute; rpm) is controlled, which affects the film thickness and morphology. The spinning process is completed through the repetition of these steps: (a) spinning the sol (~3000 rpm/min for 30 s) on the substrate, (b) drying at low temperature (120°C for 10 min), (c) drying at relatively high temperature (350°C for 10 min), (d) drying in a furnace in the temperature range ~ 500–600°C for 10 min. The steps from (a) to (d) are reported as the preheat treatment process in literature. The parameters, such as drying time and temperatures, can be varied. After applying various layers by the same procedure, the films are annealed (referred as post-heating) at selected temperatures for longer dwell time to develop homogeneous, crystalline, and single phase ZnO films. The annealing regime affects the grain growth and the crystalline microstructure of the ZnO films [37]. **Table 2** presents various sol-gel methodologies recently reported for the ZnO film processing.

Precursor (mol L ⁻¹)	Alcohol	Additive	Aging (h)	Substrate	Ph-T ^a (°C)	Po-T ^b (°C)	Thickness (nm)	Cryst. orientation	Ref.
ZAD (0.4)	MeOH EtOH PrOH 2-ME	2-Ma MEA DEA	–	Si ₍₁₀₀₎	140–170	400	–	(100), (002) , (101)	[27]
ZAD	EtOH PrOH	MEA	15	Quartz	300	500	175–200	(100), (002) , (101), (102), (110), (103), (112), (004)	[29]
ZAD (0.6)	PrOH	MEA	24	Glass	300	500	–	(100), (002) , (101), (102), (110)	[38]
ZAD (0.1)	EtOH	MEA	24	Soda-lime Silica Silicon Pt _(50 nm) / Ti _(5 nm) / SiO ₂	250	400	140	(100), (002), (101)	[30]
ZNH (0.3)	PrOH	MMEA	120	Sapphire	700	700	300–1900	(100), (002), (101)	[28]
ZNH (0.3)	PrOH	MEA	168	Sapphire	300–600	600	–	(100), (002), (101) or (100), (002) , (101)	[39]
ZAD (0.75)	EtOH	MEA	–	Glass	200	500	–	(100), (002) , (101)	[40]
ZAD (0.5)	EtOH	MEA	–	Glass	100	450, 600	–	(100), (002) , (101), (102)	[41]
ZAD	MeOH PrOH	MEA	24	SiO ₂ /Si	150	500	–	(100), (002) , (101) or (100), (002), (101)	[42]
ZAD (0.2-0.1)	2-ME	MEA	24	Glass	300	500	180–270	(100), (002) , (101), (102), (110)	[31]

Precursor (mol L ⁻¹)	Alcohol	Additive	Aging (h)	Substrate	Ph-T ^a (°C)	Po-T ^b (°C)	Thickness (nm)	Cryst. orientation	Ref.
ZAD	EtOH MeOH BD PrOH	MEA	840	Glass	190	550	–	(100), (002) , (101)/ (100), (002) , (101)/ (100), (002) , (101)/ (100), (002) , (101)/ (100), (002) , (101)	[43]
ZAD (0.2)	EtOH	MEA	72	Glass	230	450	98–366	(100), (002) , (101)	[44]
ZAD (0.5)	PrOH	DEA	–	Glass	25 (RT)	450	311	(100), (002), (101) , (102), (110), (103), (200), (112), (201), (004), (202)	[32]
ZAD (0.1–0.5)	2-ME	MEA	–	Quartz	170–350	250–400	–	(100), (002) , (101)	[45]
ZAD (0.1)	PrOH	DEA	–	Glass	550	400	350	(100), (002) , (101)	[46]
ZAD (0.2)	PrOH	MEA DEA TEA TE EN	–	Soda lime Glass	120–300	500	300–370	(10 ⁻¹⁰), (0002) , (10 ⁻¹¹)	[35]
ZAD	EtOH -water	AcA	–	SiO ₂	200	450	–	(100), (002), (101)	[47]
ZAD (0.75)	2-ME	MEA	24	Sapphire	300	600–900	50–350	(100), (002) , (101), (102), (110), (103), (112)	[48]

Precursor (mol L ⁻¹)	Alcohol	Additive	Aging (h)	Substrate	Ph-T ^a (°C)	Po-T ^b (°C)	Thickness (nm)	Cryst. orientation	Ref.
ZAD (0.3)	2-ME / PEG	MEA	24	Glass	300	600	257–277	(100), (002) , (101), (102), (110), (103)	[49]
ZAD	2-ME	TEA	36	Glass	500	600	230–350	(100), (002) , (101), (102), (110), (103), (112)	[50]
ZAD (0.75)	EtOH	MEA	–	Glass	200	500	–	(100), (002) , (101)	[51]
ZAD (0.1–0.3)	PrOH	MEA	24	Soda lime glass	80	400	218–437	(10 ⁻¹⁰), (0002) , (10 ⁻¹¹)	[52]
ZAD	2-ME	MEA	–	SiO ₂ /Si	200	500	–	(100), (002) , (101), (102), (110), (103), (112)	[53]
ZAD (0.5)	2-ME	MEA	–	Si-wafer	300	500–900	–	(002)	[54]
ZAD (0.5)	2-ME	DEA	168	Glass	300	500	170	(100), (002), (101) , (102), (110), (103)	[3]
ZAD	MeOH	–	720	Glass	180	400–500	–	(100), (002), (101) , (102), (110), (103), (200)	[55]
ZAD (0.09–0.75)	2-ME	MEA	–	Si ₍₀₀₁₎	300	500	24–94	–	[56]

Abbreviation	Product name	Formula	Abbreviation	Product name	Formula
ZAD	Zinc acetate dihydrate	Zn(CH ₃ COO) ₂ ·2H ₂ O	MeOH	Methanol	CH ₃ OH
ZNH	Zinc nitrate hexahydrate	Zn(NO ₃) ₂ ·6H ₂ O	EtOH	Ethanol	C ₂ H ₅ OH

Abbreviation	Product name	Formula	Abbreviation	Product name	Formula
2-ME	2-Methoxyethanol	CH ₃ O(CH ₂) ₂ OH	PrOH	<i>x</i> -Propanol	C ₃ H ₇ OH
TE	Triethylamine	N(CH ₂ CH ₃) ₃	ED	Ethylenediamine	C ₂ H ₄ (NH ₂) ₂
DEA	Diethanolamine	(HOCH ₂ CH ₂) ₂ NH	AcA	Acetic acid	CH ₃ COOH
MEA	Monoethanolamine	(HOCH ₂ CH ₂) ₂ NH ₂	PEG	Polyethyleneglycol	C _{2n} H _{4n+2} O _{n+1}
TEA	Triethanolamine	(HOCH ₂ CH ₂) ₃ N	BD	1,4-butanediol	HOCH ₂ CH ₂ CH ₂ CH ₂ OH
2-Ma	2-(methylamino) ethanol	C ₃ H ₉ NO			

^aPreheat treatment; ^bpostheat treatment.

The bold entries are self explanatory which suggest the preferential crystallographic orientation.

Table 2. Recently published papers about the sol-gel-derived ZnO films.

3. Doping of ZnO

The term doping is used to introduce impurities in semiconductors. Similarly, doping mechanism is applied to improve the properties of ZnO (**Table 3**). Transition elements such as Cu²⁺, Fe³⁺, Co³⁺, Mn²⁺ are used to alter the ZnO optical and electrical properties [57]. The dopants in ZnO crystal structure affect the crystal structure, volume, lattice parameters, hopping mechanism of electron, band gap, and particle morphology, which are efficient ways in which the properties of ZnO are improved [58]. It has been reported that 9 mol% Fe in ZnO decreases the d-spacing of ZnO crystal. The ionic radius of Fe³⁺ (0.68 Å) is smaller than Zn²⁺ (0.74 Å), which can possibly influence the crystal lattice due to the generation of tension in the crystal. Further, it decreases the crystal growth. The E_g also decreases with Fe due to the addition of more energy levels, consequently resulting in defects. Aydin et al. [59] reported a corresponding decrease in E_g for the samples with 5, 10, 15, and 20% Fe-doped ZnO as 3.08, 2.83, 2.79, and 2.75 eV, respectively. Xu and Li [60] processed sol-gel-derived Fe-ZnO on the Si substrates. The preferential orientations of the film perpendicular to the substrate surface along the *c*-axis and the crystalline nature were reported to increase for the 1% Fe doping concentration. However, with increasing Fe from 1% worsen the above-mentioned properties. The grain size was also decreased with increasing Fe content. The E_g was observed to increase. Aluminum (Al³⁺; ionic radii: 0.053 nm) doping in Zn²⁺ (0.074 nm) decreases the interplanar d-spacing and lattice constants [61]. Chen et al. [62] investigated the effect of Ga-ZnO film thickness (230–480 nm), temperature (400–600°C) and atmosphere (air/argon) to improve the optical response and electronic microstructure of the ZnO. The films were processed by using the sol-gel dip coating technique, where thick films showed high crystalline nature. The annealing atmosphere resulted in the low carrier concentration, while an increase in the particle size promoted the carrier concentration. The argon atmosphere possibly produced films exhibiting resistivity $1.18 \times 10^{-2} \Omega \text{ cm}$, carrier density ($3.376 \times 10^{19} \text{ cm}^{-3}$), and mobility ($15.74 \text{ cm}^2 \text{ (Vs)}^{-1}$). Dubey et al. [63] used Mn and Li as the co-dopants to optimize the optical and magnetic behavior of ZnO thin films, which were processed through a sol-gel route according to the stoichiometric formula Zn_{1-y-x}Mn_yLi_xO ($y = 0, 0.02 | x = 0-0.06$). The lattice parameters were observed to increase linearly and were associated with the distortion

Dopant	Conc. (%)	Substrate	Annealing (°C)	Atm.	ρ (Ω cm)	E_g (eV)	Application	Ref.
Al	24.71	p-type Si	500	H ₂			Solar cells	[65]
Ti	0.5	Glass	400	Air	3.8×10^{-4}	3.346	Transparent cond. layer	[66]
Fe	1–5	borofloat glass	650	Air		3.371		[67]
Cu	0.00, 0.03, 0.06, 0.10	Si ₍₁₀₀₎	750	Air		3.22–3.43	Optical	[68]
Sn-Al			500	Air/ Vacuum	0.52–575.25	3.28–3.32	Optoelectronic	[69]
Co	0–10	Corning glass	550	Air		3.26–3.31	Magnetic	[70]
Na	3–30	Quartz glass	800	Air		3.25–3.293	Optical	[71]
Ru	0–6	Si/Quartz	600			3.278–3.372	Transistors	[72]
Li	0–0.2		500	Air			Sensors	[73]
Al-Ni	1.5	Corning glass	450–600	N ₂ /H ₂	1.05×10^{-3} – 6.53×10^{-3}		Optoelectronic	[74]
Al B	0.25–5.0 0.25–1.25	Glass	550	Air/ 5% N ₂ /95% H ₂	1.99×10^{-3} 4.01		Optoelectronic	[75]
Al		Quartz	600	Air	3.22–1.42	3.21–3.14	Gas sensing	[76]
Fe	1–4	FTO	450	–		3.26–3.21	Optical	[77]
In	3	Quartz	600	Air			Sensing	[78]
Mn	1–5	Glass	400	Air		3.43	Optical	[79]
Cu	1–4	Glass	500	–			Sensing	[80]
Ga	0–1	Alkali free glass	550			3.27–3.29	Sensing	[81]
Ag	0–3	Glass	500	Air		3.31–3.69	Optical	[82]
Al	0–12	Glass	300–500	Air			Optoelectronic	[83]
Fe	0–20	Glass	500			3.07–3.38	Optoelectronic/ Magnetic	[84]
Li	0.25–1.25	Glass	450	Air			Optoelectronic Thermal	[85]
Pb	1–4	Glass	500			3.19–3.25	Optoelectronic	[86]
Al-Ti	(1)Al–(0.1)Ti	Glass	550	Air	900×10^6 – 13×10^6	3.23–3.26	Optical	[87]
Co	0–0.09	Quartz glass	650	Air		3.26–3.28	Optical	[88]
Mn	0–12	Glass	450	Air		3.89–3.15	Optical	[89]
B	0–5	Alkali free glass	500		2.2×10^2	3.25–3.3	Optical	[90]
Ga	0–3	Glass	500	Vacuum	102–9	3.24–3.28	Photocatalytic	[91]

Table 3. Recently used impurities in the ZnO films for different applications.

of the Zn tetrahedron. The Mn K-edge XANES data revealed the Mn^{2+} in the 2% Mn-doped samples, while the oxidation state was reported as Mn^{2+} and Mn^{3+} in the co-doped samples. Furthermore, the methylene blue dye degradation was improved up to 90% with the co-doping mechanism. All the samples showed a preferred crystallographic orientation (100), (002), (101), (102), (110), (103), (112), and (210). The crystallite size calculated using a Scherrer equation was observed to increase nonlinearly from 27.180 to 27.145 nm for the undoped to high doped samples, respectively. Vijayaprasath et al. [64] used various transition metals (Ni, Mn, Co = 0.03 mol%) as impurities in the ZnO crystal lattice by processing sol-gel-derived pure and doped ZnO films. The X-ray diffraction (XRD) studies confirmed the hexagonal wurtzite structure with (002) preferred orientation. Optical characterization showed a transparent character in the visible region while a d-d transition was reported in the violet region, which was associated with the crystalline defects and grain morphology. The crystalline size was reported as 28.70, 27.74, 26.00 and 27.74 nm for the pure ZnO, Ni-, Mn-, and Co-doped ZnO, respectively. An increase in the dislocation density (lines m^{-2}) and microstrain (lines⁻² m^{-4}) was observed for all the transition elements. The resultant films exhibited well-defined ferromagnetic properties at room temperature. The coercivity of Ni-, Mn-, and Co-doped ZnO thin films was 41, 58 and 49 Oe (Oersted), respectively. It is important to further investigate the effect of elements in the ZnO both theoretically and experimentally. The new mechanism that can potentially improve the properties of ZnO is the co-doping mechanism rarely reported.

4. Application of ZnO

Zinc oxide has been utilized as a potential technological material for centuries. In the Bronze age, the smelting process for copper ore produced ZnO as a by-product. It was also used for the wounds healing and brass (Cu-Zn alloy) production. After industrialization in the mid-nineteenth century, ZnO was used in white paint, rubber vulcanization activation, and porcelain enamels. In the following, we will discuss comprehensive details of the selected electronic and optical applications of ZnO.

4.1. Gas sensing

ZnO nanostructures have been extensively studied for use in gas sensing applications. A gas sensor is designed to convert chemical information (concentration) of a particular gas present in a designated space into an electric (or optical) signal (**Figure 4**). The basic requirements of such a device configuration are: (1) compaction in order to install it in a commodity appliance and (2) must be economical. In principle, the gas sensors are designed by combining two key functions. The first one is the gas recognition, which is conducted through adsorption, reduction or electrochemical reactions to/by sensor materials or electrode (receptors). The second function is the transduction of this information in the form of signals (signal transduction). The interaction can be any physical or chemical effect on or around the receptors, such as a reaction product, adsorbed formations, generation of heat of reactions, changes in receptors mass, dimensions, surface/bulk properties and changes in the electrode potentials.

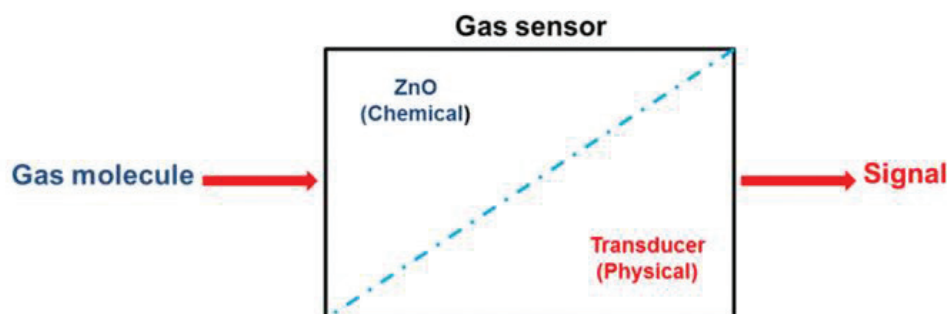
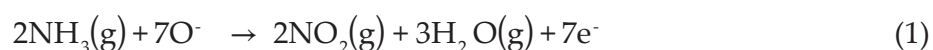


Figure 4. A typical ZnO-based gas sensor.

In the case of semiconductors, the changes in the work function are monitored, and consequently, the work function dependent resistance is monitored. The surface conductivity of the ZnO is recorded in response to the adsorbed gas. As mentioned in the previous text, the surface of the ZnO exhibits the point defects, which affect the conductivity of ZnO. The oxygen vacancies are dominant defects in ZnO that are generally generated in the films by annealing at high temperature. The resistance of ZnO-based sensors is monitored, which correspond to the adsorption and desorption of the target gas molecule on the surface of the sensors [92]. The surface of ZnO captures oxygen from the air, which is converted into oxygen ions by taking electrons from the conduction band. This phenomenon results in decreasing the charge carrier species, subsequently resulting in increasing the resistance across the circuit. For example, when ammonia molecules react with O_2 on the surface, the electrons flow back into the conduction band which decreases the circuit resistance. The oxygen and NH_3 reaction are as follows:



The gas sensing properties of ZnO depend on the surface areas, porosity, defect concentration, and working temperature. The thickness of the ZnO film by sol-gel route is controlled by varying the sol-gel concentrations and deposition cycles. Kumar et al. [44] reported that an increase in the film thickness from 98 to 366 nm resulted in particle size growth and surface roughness 5.8–47 nm, respectively. Further, the band gap was observed to decrease from 3.33 to 3.24 eV, respectively. Films with high surface roughness showed good gas sensing characteristics. Huo and Jayatissa [93] studied the effect of laser irradiation on the sol-gel-derived ZnO film thickness and H_2 sensing. A pulsed laser ($\lambda = 532$ nm, pulsed rate = 8 nm, pulsed $f = 5$ kHz, laser fluence range = 1.06–3.58 J/cm²) was used in this experiment. The low irradiation promoted the grain growth and crystallinity, while the high-dose resulted in deterioration of the crystallinity. The H_2 sensing ability of the Al-doped ZnO was observed to be dependent on the film thickness and optimum dose of the laser. Liu et al. [76] reported the sensing and optical properties for the Al-doped ZnO films deposited on the quartz substrates and annealed with a different heating process. The films exhibited $E_g = 3.21$ –3.14 eV, resistivity = 3.22–1.42 Ω cm, average transmittance 400–700 nm increased from 82.9 to 86.7%. The sensing properties were in ethanol atmosphere. The thin films showed high response and recovery toward ethanol gas sensing. Hou et al. [94] utilized two different Zn metal salts (Zinc acetate and Zinc nitrate) to develop Al-doped ZnO films. These precursors were selected as

the controlling factors to investigate its effect on the films microstructure, conductivity, and gas sensing response for the Zinc acetate compared to the Zn-nitrate. Different concentrations of the hydrogen in the air were also investigated. Zinc acetate-derived films exhibited a skeletal wrinkles structure. The sample with 3.0% Al-doped ZnO showed conductivity, high tunability for a selective, and optimum operating temperatures.

4.2. Photocatalytic applications

The photocatalysis process can be exploited as a renewable energy source and an environmental technology for application ranging from solar cell to photoelectrochemical cells for water splitting reactions, purification of hazardous materials from industrial effluents, that is, removal/degradation of drugs, dye, and conversion of alcohols to fuel. The photocatalysis is an important electrochemical process, which occurs under light irradiations either from the sun or artificial light source that occurs at the surface of a photocatalyst (semiconductor material). The interaction of photon to the photocatalyst is a very important characteristic that facilitates/deteriorate the photocatalytic process. The photocatalysts have been under extensive investigations, and recently, a number of efforts have been given to tune the electronic microstructure of the semiconductor materials. For this purpose, efforts have been made not only to modify the synthesis procedures, but also the crystal orientations, impurities, tuning the defect chemistry such as TiO_2 . However, there is still room to improve the photocatalysts for industrial applications and to understand the physical and chemical processes involved [95]. ZnO is one of the efficient photocatalysts that exhibit good photocatalytic activity, non-toxicity, and abundance [96]. The environmental contaminants are degraded by using ZnO as the photocatalysts. When the energy of the incident photons is equal to or greater than the E_g energy of the ZnO, reactive species such as H_2O_2 , Radicles (i.e., anions ($\cdot\text{O}^{2-}$) and hydroxyl ($\cdot\text{OH}$)) are produced, which are strong oxidizing agents that facilitate the photocatalytic process of degrading the organic and pharmaceutical pollutants. Moreover, these reactive species can be used as antibacterial agents that can rupture the outer membrane of bacteria, inhibiting their growth. The antibacterial agents can be organic or inorganic; however, the inorganic antibacterial agents are more stable and safe. ZnO is categorized as the most promising inorganic antibacterial agent that showcase antibacterial activity, even in the absence of UV light. These properties can be exploited for various applications, such as wastewater treatment. Additionally, the thin ZnO films exhibiting antibacterial activity can be used to modify windows in buildings for protection purposes against certain microbes. Recently, the self-healing films with good antibacterial activity are under consideration to improve health care facilities for the public [97]. The ZnO is applied in the form of aqueous slurries as a photocatalyst; however, the process is technologically not feasible, and thus, it cannot be used to recycle and recover the catalyst after wastewater treatment. To overcome this issue, attempts have been reported to develop ZnO thin films on rigid substrates such as glass (beads, fibers), aluminum foil sheet, and stainless steel. The photocatalytic response of these films is lower compared to the nanopowders. A new approach is to develop immobilized nanostructured photocatalysts, exhibiting superior microstructure properties such as a high number of active sites and surface to volume ratio compared to thin films. Furthermore, mixed phases are fabricated to increase the photocatalytic activity. Georgakopoulos et al. [98] processed the $\text{TiO}_2/$

ZnO nanocomposites and studied the photoconductivity of various stoichiometric ratios both in vacuum and in air. The environment did not affect the photoconductivity amplitudes; however, a high decay rate was recorded in the air. Moreover, a composite ZnO (10%)/TiO₂ thin film degraded 78.1% of methyl orange (MO) compared to pure TiO₂ (49.3%) [99]. Despite absorption in the ultraviolet region of the solar spectrum by ZnO, for good photocatalytic properties, it is important that ZnO absorbs the visible region because the solar spectrum constitutes only 5–7% UV light, while the visible and IR percentage are higher 46 and 47%, respectively. Therefore, the E_g of the ZnO is narrowed by doping the transition elements to improve the absorption of the visible region of the solar spectrum [100]. Davar et al. [101] adopted a novel green chemistry route to develop ZnO for the degradation of various dyes such as methyl blue (MB), methyl red (MR), and methyl orange. The effect of sucrose solution was added in various ratios to investigate its effect on the lemon juice and zinc acetate solutions. The product materials studied by SEM and XRD showed an enhanced grain morphology and crystal phase. The as-synthesized ZnO showed a good photocatalytic response to the degradation of various dyes used in this work, and the photocatalyst can also be used for commercial applications in the degradation of dyes in the textile industry.

4.3. Thermoelectric properties

The demands for the generation of energy from sources that are free from carbon emission are increasing which has a great impact on the current social economic and political structure. The production of energy from sources such as fossil fuels and natural gas has increased the production of carbon dioxide emission in the atmosphere and sulfur compounds to an alarming rate, which poses a great threat to our environment and health. To overcome these issues, attempts have been made to produce energy from clean sources and utilize alternative means of energy. These include sources like hydrogen fuel economy, solar cells, piezoelectric materials, pyroelectric materials, and thermoelectric materials for energy harvesting either from sun radiations, vibrations and movements or, surrounding heat and heat generated in the automobiles and industries. Every year a tremendous amount of energy is wasted in the form of heat, which provides an opportunity to harness the energy for power generation. Techniques have been explored to recover waste heat, such as Organic Rankine Cycle (ORC), which utilizes an organic fluid, using superheated gases for running blades in a turbine for power generation, and thermoelectric generators, those can transfer the difference of heat energy between the two plates into a DC power by using Seebeck, Peltier, and Thomson effect, which can be exploited for the generation of electric powers from heat. In the past few years, many materials, both oxide and non-oxide-based, have been studied to improve the performance of the TEGs. The non-oxide-based TEGs have better ZT values; however, they contain lead and other heavy and expensive metals, which cannot be used for large-scale implementation. The oxide-based TEGs are cheap, abundant and have the potential to improve its properties by tuning the defect chemistry and conductivity in these materials. Further, these materials are more stable at high temperature compared to non-oxide based, which readily oxidizes at extreme temperature and deteriorate its properties. ZnO is considered to be one of the potential thermoelectric materials, which has recently gained attention due to its stability and economy. TEGs are based on p- and n-type semiconductor materials connected in series and parallel to

deal with current and heat flow, respectively. The thermoelectric figure of merit, $ZT = S^2\sigma T/\kappa$ where T is the temperature, S is the Seebeck coefficient, σ is the electrical conductivity, and κ is the thermal conductivity, is the measure of the potential efficiency of a thermoelectric material [102]. The thermoelectric power factor (PF) of ZnO is comparatively higher and can be used as alternatives to the conventional thermoelectric materials. The PF is given as $ZT^{1/4}(rS^2T)/k$, where r is defined as electrical conductivity. The doping mechanism can be adopted in ZnO to restructure the crystal architecture, which can possibly increase r . In such a way, the semiconductor behavior can be changed into a metallic one. The Al doping has been reported to increase the magnitude of r by the three order; however, the high k results in a low thermoelectric performance. The thermoelectric properties can be improved by improving the electronic transport mechanism [103]. Liang [103] reported the effect of Fe on the ZnO for thermoelectric applications. The XRD confirmed the ZnO solid solution and ZnFe_2O_4 spinel phases. The magnitude of ZT was observed to increase with increasing Fe concentration, which might be associated with phonon scattering, point defects, and electron transport mechanism.

5. Summary and future perspectives

This chapter reviewed the processing, effect of doping, and strategies to improve the development of the sol-gel derived pure and doped ZnO films, with an emphasis understanding the parameters that can influence the optical and electronic properties of these materials. Moreover, it has been discussed how these materials can be used for gas sensing, photocatalytic and thermoelectric applications. The number of publications on sol-gel chemistry is increasing every year, which shows its potentials in semiconductor-based films processing that can be exploited and applied on an industrial scale. The doping mechanism, film microstructure, and hence the final properties can be easily controlled by the sol-gel method; however, the parameters, which can influence the properties and durability of the sol-gel derived films, must be further investigated and optimized. For instance, very little attention has been given to understand the film growth and grain orientation on the nanoscale, and most of the studies generalize/overlook this approach. It is important to modify the sol-gel process to develop the homogeneous ZnO-based films with preferred crystal orientations and controlled microstructure, which can be proved as an alternative to atomic layer deposition and magnetron sputtering techniques. Few studies report the microstructure evaluation, which limits the usefulness of sol-gel for the sensitive and reliable applications. Future studies must focus on the grain formation in sol-gel during film processing and crystal orientation mechanism must be studied, which will open a new window in the sol-gel regime. Moreover, the grain-to-grain connection and density parameters must be investigated in detail, which strongly affect the electrical properties of the device. Although the sol-gel technology for the semiconductor processing has been used for decades, the methods have been overlooked. Despite hundreds of papers published each year, the sol-gel process has been little modified, that is, sol-precipitation and sol-hydrothermal method. The major issues, which are not only related to the current discussion, but also, in general, are the reproducibility of the results which are reported differently from lab to lab. The percentage of reproducibility of the experimental results reported is extremely low, which demolishes the adoption of such techniques.

The importance of the sol-gel technology and further modification in the techniques will increase in the near future. The new precursors and developing new sol-gel chemistry will change the film growth technology, and sol-gel has enormous potential for commercial applications. Sol-gel-derived films will generate unique properties to cope with the needs of future technological device applications.

Author details

Asad Mahmood and Abdul Naeem*

*Address all correspondence to: naeem@upesh.edu.pk

National Centre of Excellence in Physical Chemistry, University of Peshawar, Pakistan

References

- [1] Pal D, Mathur A, Singh A, Singhal J, Sengupta A, Dutta S, Sudeshna SZ. Tunable optical properties in atomic layer deposition grown ZnO thin films. *Journal of Vacuum Science & Technology A: Vacuum, Surfaces, and Films*. 2017;35: 01B108. doi:10.1116/1.4967296
- [2] Hoye RLZ, Muñoz-Rojas D, Nelson SF, Illiberi A, Poodt P, Roozeboom F, Judith L. Research Update: Atmospheric pressure spatial atomic layer deposition of ZnO thin films: Reactors, doping, and devices. *APL Materials*. 2015;3: 040701. doi:10.1063/1.4916525
- [3] Tsay C-Y, Lee W-C. Effect of dopants on the structural, optical and electrical properties of sol-gel derived ZnO semiconductor thin films. *Current Applied Physics*. 2013;13: 60–65. doi:10.1016/j.cap.2012.06.010
- [4] Wang ZL. Zinc oxide nanostructures: growth, properties and applications. *Journal of Physics: Condensed Matter* 1. 2004;16: R829–R858
- [5] Kresse G, Hafner J. Ab initio molecular dynamics for liquid metals. *Physical Review B*. 1993;47: 558–561. doi:10.1103/PhysRevB.47.558
- [6] Alias SS, Mohamad AA. ZnO nanocrystalline metal oxide semiconductor via sol gel method. *SpringerBriefs in Materials*. 2014: 1–8. doi:10.1007/978-981-4560-77-1_1
- [7] Saha D, Misra P, Das G, Joshi MP, Kukreja LM. Observation of dopant-profile independent electron transport in sub-monolayer TiO_x stacked ZnO thin films grown by atomic layer deposition. *Applied Physics Letters*. 2016;108: 032101. doi:10.1063/1.4939926
- [8] Kaushik VK, Mukherjee C, Ganguli T, Sen PK. Material characterizations of Al:ZnO thin films grown by aerosol assisted chemical vapour deposition. *Journal of Alloys and Compounds*. 2016;689: 1028–1036. doi:10.1016/j.jallcom.2016.08.022
- [9] Kumar V, Ntwaeaborwa OM, Swart HC. Deep level defect correlated emission and Si diffusion in ZnO:Tb(3+) thin films prepared by pulsed laser deposition. *Journal of Colloid and Interface Science*. 2016;465: 295–303. doi:10.1016/j.jcis.2015.12.007

- [10] Suzuki T, Chiba H, Kawashima T, Washio K. Comparison study of V-doped ZnO thin films on polycarbonate and quartz substrates deposited by RF magnetron sputtering. *Thin Solid Films*. 2016;605: 53–56. doi:10.1016/j.tsf.2015.11.064.
- [11] Demiroglu I, Bromley ST. Evidence for multi-polymorphic islands during epitaxial growth of ZnO on Ag(111). *Journal of Physics Condensed Matter : An Institute of Physics Journal*. 2016;28: 224007. doi:10.1088/0953-8984/28/22/224007
- [12] Zhang B, Wang F, Zhu C, Li Q, Song J, Zheng M, Ma L, Shen W. A facile self-assembly synthesis of hexagonal zno nanosheet films and their photoelectrochemical properties. *Nano-Micro Letters*. 2016;8: 137–142. doi:10.1007/s40820-015-0068-y
- [13] Kunj S, Sreenivas K. Near band edge emission characteristics of sputtered nano-crystalline ZnO films. *Proceeding of International Conference on Condensed Matter and Applied Physics (ICC 2015)*. 2016;1728: 020520. doi:10.1063/1.4946571
- [14] El-Shazly AN, Rashad MM, Abdel-Aal EA, Ibrahim IA, El-Shahat MF, Shalan AE. Nanostructured ZnO photocatalysts prepared via surfactant assisted co-precipitation method achieving enhanced photocatalytic activity for the degradation of methylene blue dyes. *Journal of Environmental Chemical Engineering*. 2016;4: 3177–3184. doi:10.1016/j.jece.2016.06.018
- [15] Kıcı N, Tüken T, Erken O, Gumus C, Ufuktepe Y. Nanostructured ZnO films in forms of rod, plate and flower: Electrodeposition mechanisms and characterization. *Applied Surface Science*. 2016;377: 191–199. doi:10.1016/j.apsusc.2016.03.111
- [16] Rajah S, Barhoumi A, Mhamdi A, Leroy G, Duponchel B, Amlouk M, Guermazi S. Structural, morphological, optical and opto-thermal properties of Ni-doped ZnO thin films using spray pyrolysis chemical technique. *Bull Mater Sci*. 2016;39: 177–186.
- [17] Duan L, Zhao X, Zhang Y, Shen H, Liu R. Fabrication of flexible Al-doped ZnO films via sol-gel method. *Materials Letters*. 2016;162: 199–202. doi:10.1016/j.matlet.2015.10.023
- [18] Yu Y, Pan W, Guo X, Gao L, Gu Y, Liu Y. A poly(arylene ether sulfone) hybrid membrane using titanium dioxide nanoparticles as the filler: Preparation, characterization and gas separation study. *High Performance Polymers*. 2017, 29(1) 26–35. doi:10.1177/0954008315626990
- [19] Barczak M, McDonagh C, Wencel D. Micro- and nanostructured sol-gel-based materials for optical chemical sensing (2005–2015). *Microchimica Acta*. 2016;183: 2085–2109. doi:10.1007/s00604-016-1863-y
- [20] Ong X, Zhi M, Gupta S, Chan Y. Wet-chemically synthesized colloidal semiconductor nanostructures as optical gain media. *Chemphyschem : A European Journal of Chemical Physics and Physical Chemistry*. 2016;17: 582–597. doi:10.1002/cphc.201500975
- [21] Mikosch A, Ciftci S, Kuehne AJ. Colloidal crystal lasers from monodisperse conjugated polymer particles via bottom-up coassembly in a sol-gel matrix. *ACS Nano*. 2016;10: 10195–10201. doi:10.1021/acsnano.6b05538

- [22] Lee S-W, Kim H, Kim M-S, Youn H-C, Kang K, Cho B-W, Roh KC, Kim KB. Improved electrochemical performance of $\text{LiNi}_{0.6}\text{Co}_{0.2}\text{Mn}_{0.2}\text{O}_2$ cathode material synthesized by citric acid assisted sol-gel method for lithium ion batteries. *Journal of Power Sources*. 2016;315: 261–268. doi:10.1016/j.jpowsour.2016.03.020
- [23] Adachi K, Tokushige M, Omata K, Yamazaki S, Iwadate Y. Kinetics of coloration in photochromic tungsten(VI) oxide/silicon oxycarbide/silica hybrid xerogel: Insight into cation self-diffusion mechanisms. *ACS Applied Materials & Interfaces*. 2016;8: 14019–14028. doi:10.1021/acsami.6b04115
- [24] Mohana Priya S, Geetha A, Ramamurthi K. Structural, morphological and optical properties of tin oxide nanoparticles synthesized by sol-gel method adding hydrochloric acid. *Journal of Sol-Gel Science and Technology*. 2016;78: 365–372. doi:10.1007/s10971-016-3966-7
- [25] Ullah A, Ahn CW, Hussain A, Kim IW. The effects of sintering temperatures on dielectric, ferroelectric and electric field-induced strain of lead-free $\text{Bi}_{0.5}(\text{Na}_{0.78}\text{K}_{0.22})_{0.5}\text{TiO}_3$ piezoelectric ceramics synthesized by the sol-gel technique. *Current Applied Physics*. 2010;10: 1367–1371. doi:10.1016/j.cap.2010.05.004
- [26] Kumar A, Gaurav, Malik AK, Tewary DK, Singh B. A review on development of solid phase microextraction fibers by sol-gel methods and their applications. *Analytica Chimica Acta*. 2008;610: 1–14. doi:10.1016/j.aca.2008.01.028.
- [27] Guo D, Ju Y, Fu C, Huang Z, Zhang L. (002)-oriented growth and morphologies of ZnO thin films prepared by sol-gel method. *Materials Science-Poland*. 2016;34: pp. 555–563 doi:10.1515/msp-2016-0076
- [28] Chia CH, Tsai WC, Chiou JW. Thickness effect on luminescent properties of sol-gel derived ZnO thin films. *Journal of Luminescence*. 2013;136: 160–164. doi:10.1016/j.jlumin.2012.11.019
- [29] Popa M, Mereu RA, Filip M, Gabor M, Petrisor TJr, Ciontea L, Petrisor T. Highly c-axis oriented ZnO thin film using 1-propanol as solvent in sol-gel synthesis. *Materials Letters*. 2013;92: 267–270. doi:10.1016/j.matlet.2012.10.099
- [30] Ayana DG, Ceccato R, Collini C, Lorenzelli L, Prusakova V, Dirè S. Sol-gel derived oriented multilayer ZnO thin films with memristive response. *Thin Solid Films*. 2016;615: 427–436. doi:10.1016/j.tsf.2016.07.025
- [31] Malek MF, Mamat MH, Sahdan MZ, Zahidi MM, Khusaimi Z, Mahmood MR. Influence of various sol concentrations on stress/strain and properties of ZnO thin films synthesised by sol-gel technique. *Thin Solid Films*. 2013;527: 102–109. doi:10.1016/j.tsf.2012.11.095
- [32] Das S, Bhattacharjee K, Maitra S, Das GC. Effect of oxygen partial pressure on the photoluminescence properties of sol-gel synthesized nano-structured ZnO thin films. *Thin Solid Films*. 2014;550: 65–70. doi:10.1016/j.tsf.2013.10.045.
- [33] Zahn M, Ohki Y, Fenneman DB, Gripshover RJ, Gehman VH. J. Dielectric properties of water and water/ethylene glycol mixtures for use in pulsed power system design. *Proceedings of the IEEE*. 1986;74: 1182–1221.

- [34] Naik GV, Bhat N. Poly-ols based sol-gel synthesis of zinc oxide thin films. *Journal of The Electrochemical Society*. 2011;158: H85. doi:10.1149/1.3515894
- [35] Hosseini Vajargah P, Abdizadeh H, Ebrahimifard R, Golobostanfard MR. Sol-gel derived ZnO thin films: Effect of amino-additives. *Applied Surface Science*. 2013;285: 732–743. doi:10.1016/j.apsusc.2013.08.118
- [36] Znaidi L. Sol-gel-deposited ZnO thin films: A review. *Materials Science and Engineering: B*. 2010;174: 18–30. doi:10.1016/j.mseb.2010.07.001
- [37] Patil SL, Chougule MA, Pawar SG, Raut BT, Sen S, Patil VB. New process for synthesis of ZnO thin films: Microstructural, optical and electrical characterization. *Journal of Alloys and Compounds*. 2011;509: 10055–10061. doi:10.1016/j.jallcom.2011.08.030
- [38] Mahroug A, Boudjadar S, Hamrit S, Guerbous L. Structural, optical and photocurrent properties of undoped and Al-doped ZnO thin films deposited by sol-gel spin coating technique. *Materials Letters*. 2014;134: 248–251. doi:10.1016/j.matlet.2014.07.099
- [39] Chia CH, Tsai WC, Chou WC. Preheating-temperature effect on structural and photoluminescent properties of sol-gel derived ZnO thin films. *Journal of Luminescence*. 2014;148: 111–115. doi:10.1016/j.jlumin.2013.12.006
- [40] Boudjouan F, Chelouche A, Touam T, Djouadi D, Khodja S, Tazerout M, Ouerdane Y, Hadjoub Z. Effects of stabilizer ratio on photoluminescence properties of sol-gel ZnO nano-structured thin films. *Journal of Luminescence*. 2015;158: 32–37. doi:10.1016/j.jlumin.2014.09.026
- [41] Benramache S, Benhaoua B, Chabane F, Guettaf A. A comparative study on the nano-crystalline ZnO thin films prepared by ultrasonic spray and sol-gel method. *Optik - International Journal for Light and Electron Optics*. 2013;124: 3221–3224. doi:10.1016/j.ijleo.2012.10.001
- [42] Foo KL, Kashif M, Hashim U, Ali ME. Sol-gel derived ZnO nanoparticulate films for ultraviolet photodetector (UV) applications. *Optik-International Journal for Light and Electron Optics*. 2013;124: 5373–5376. doi:10.1016/j.ijleo.2013.03.120
- [43] Talebian N, Nilforoushan MR, Maleki N. Ultraviolet to visible-light range photocatalytic activity of ZnO films prepared using sol-gel method: The influence of solvent. *Thin Solid Films*. 2013;527: 50–58. doi:10.1016/j.tsf.2012.11.138
- [44] Kumar V, Singh N, Mehra RM, Kapoor A, Purohit LP, Swart HC. Role of film thickness on the properties of ZnO thin films grown by sol-gel method. *Thin Solid Films*. 2013;539: 161–165. doi:10.1016/j.tsf.2013.05.088
- [45] Guo D, Sato K, Hibino S, Takeuchi T, Bessho H, Kato K. Low-temperature preparation of (002)-oriented ZnO thin films by sol-gel method. *Thin Solid Films*. 2014;550: 250–258. doi:10.1016/j.tsf.2013.11.004.

- [46] Nehmann JB, Ehrmann N, Reineke-Koch R, Bahnemann DW. Aluminum-doped zinc oxide sol-gel thin films: Influence of the sol's water content on the resistivity. *Thin Solid Films*. 2014;556: 168–173. doi:10.1016/j.tsf.2014.01.052.
- [47] Heredia E, Bojorge C, Casanova J, Cánepa H, Craievich A, Kellermann G. Nanostructured ZnO thin films prepared by sol-gel spin-coating. *Applied Surface Science*. 2014;317: 19–25. doi:10.1016/j.apsusc.2014.08.046
- [48] Cui L, Wang G-G, Zhang H-Y, Sun R, Kuang X-P, Han J-C. Effect of film thickness and annealing temperature on the structural and optical properties of ZnO thin films deposited on sapphire (0001) substrates by sol-gel. *Ceramics International*. 2013;39: 3261–3268. doi:10.1016/j.ceramint.2012.10.014
- [49] Aydemir S, Karakaya S. Effects of withdrawal speed on the structural and optical properties of sol-gel derived ZnO thin films. *Journal of Magnetism and Magnetic Materials*. 2015;373: 33–39. doi:10.1016/j.jmmm.2014.01.077
- [50] Goktas A, Mutlu IH, Yamada Y. Influence of Fe-doping on the structural, optical, and magnetic properties of ZnO thin films prepared by sol-gel method. *Superlattices and Microstructures*. 2013;57: 139–149. doi:10.1016/j.spmi.2013.02.010
- [51] Khodja S, Touam T, Chelouche A, Boudjouan F, Djouadi D, Hadjoub Z, Fischer A, Boudrioua A. Effects of stabilizer ratio on structural, morphological, optical and waveguide properties of ZnO nano-structured thin films by a sol-gel process. *Superlattices and Microstructures*. 2014;75: 485–495. doi:10.1016/j.spmi.2014.08.010
- [52] Thongsuriwong K, Amornpitoksuk P, Suwanboon S. Structure, morphology, photocatalytic and antibacterial activities of ZnO thin films prepared by sol-gel dip-coating method. *Advanced Powder Technology*. 2013;24: 275–280. doi:10.1016/j.apt.2012.07.002
- [53] Li C-F, Hsu C-Y, Li Y-Y. NH₃ sensing properties of ZnO thin films prepared via sol-gel method. *Journal of Alloys and Compounds*. 2014;606: 27–31. doi:10.1016/j.jallcom.2014.03.120.
- [54] Caglar M, Ruzgar S. Influence of the deposition temperature on the physical properties of high electron mobility ZnO films by sol-gel process. *Journal of Alloys and Compounds*. 2015;644: 101–105. doi:10.1016/j.jallcom.2015.04.167.
- [55] Quiñones-Galván JG, Sandoval-Jiménez IM, Tototzintle-Huitle H, Hernández-Hernández d LA, Moure-Flores e FD, Hernández-Hernández A, Campos-González E, Guillén-Cervantes A, Zelaya-Angel O, Araiza-Ibarra JJ. Effect of precursor solution and annealing temperature on the physical properties of sol-gel-deposited ZnO thin films. *Results in Physics*. 2013;3: 248–253. doi:10.1016/j.rinp.2013.11.001.
- [56] Guillemin S, Consonni V, Rapenne L, Sarigiannidou E, Donatini F, Bremond G. Identification of extended defect and interface related luminescence lines in polycrystalline

- ZnO thin films grown by sol-gel process. *RSC Adv.* 2016;6: 44987–44992. doi:10.1039/c6ra04634g
- [57] Janisch R, Gopal P, Spaldin NA. Transition metal-doped TiO₂ and ZnO—present status of the field. *Journal of Physics: Condensed Matter.* 2005;17: R657–R689. doi:10.1088/0953-8984/17/27/r01
- [58] Ciciliati MA, Silva MF, Fernandes DM, de Melo MAC, Hechenleitner AAW, Pineda EAG. Fe-doped ZnO nanoparticles: Synthesis by a modified sol-gel method and characterization. *Materials Letters.* 2015;159: 84–86. doi:10.1016/j.matlet.2015.06.023
- [59] Aydın C, Abd El-sadek MS, Zheng K, Yahia IS, Yakuphanoglu F. Synthesis, diffused reflectance and electrical properties of nanocrystalline Fe-doped ZnO via sol-gel calcination technique. *Optics & Laser Technology.* 2013;48: 447–452. doi:10.1016/j.optlastec.2012.11.004
- [60] Xu L, Li X. Influence of Fe-doping on the structural and optical properties of ZnO thin films prepared by sol-gel method. *Journal of Crystal Growth.* 2010;312: 851–855. doi:10.1016/j.jcrysgro.2009.12.062
- [61] Zhang Z, Bao C, Yao W, Ma S, Zhang L, Hou S. Influence of deposition temperature on the crystallinity of Al-doped ZnO thin films at glass substrates prepared by RF magnetron sputtering method. *Superlattices and Microstructures.* 2011;49: 644–653. doi:10.1016/j.spmi.2011.04.002.
- [62] Chen S, Warwick MEA, Binions R. Effects of film thickness and thermal treatment on the structural and opto-electronic properties of Ga-doped ZnO films deposited by sol-gel method. *Solar Energy Materials and Solar Cells.* 2015;137: 202–209. doi:10.1016/j.solmat.2015.02.016
- [63] Dubey DK, Singh DN, Kumar S, Nayak C, Kumbhakar P, Jha SN, Bhattacharya D, Ghosh AK, Chatterjee S. Local structure and photocatalytic properties of sol-gel derived Mn–Li co-doped ZnO diluted magnetic semiconductor nanocrystals. *RSC Adv.* 2016;6: 22852–22867. doi:10.1039/c5ra23220a
- [64] Vijayaprasath G, Murugan R, Ravi G, Mahalingam T, Hayakawa Y. Characterization of dilute magnetic semiconducting transition metal doped ZnO thin films by sol-gel spin coating method. *Applied Surface Science.* 2014;313: 870–876. doi:10.1016/j.apsusc.2014.06.093
- [65] Khan F, Baek S-H, Mobin A, Kim JH. Enhanced performance of silicon solar cells by application of low-cost sol-gel-derived Al-rich ZnO film. *Solar Energy.* 2014;101: 265–271. doi:10.1016/j.solener.2013.12.025
- [66] Eshaghi A, Hakimi MJ, Zali A. Fabrication of titanium zinc oxide (TZO) sol-gel derived nanostructured thin film and investigation of its optical and electrical properties. *Optik-International Journal for Light and Electron Optics.* 2015;126: 5610–5613. doi:10.1016/j.ijleo.2015.09.243
- [67] Ilıcan S, Özdemir Y, Caglar M, Caglar Y. Temperature dependence of the optical band gap of sol-gel derived Fe-doped ZnO films. *Optik – International Journal for Light and Electron Optics.* 2016;127: 8554–8561. doi:10.1016/j.ijleo.2016.06.074

- [68] Yang S, Zhang Y, Mo D. Spectroscopic ellipsometry studies of sol-gel-derived Cu-doped ZnO thin films. *Thin Solid Films*. 2014;571: 605–608. doi:10.1016/j.tsf.2014.02.097
- [69] Lee M-I, Huang M-C, Legrand D, Lerondel G, Lin J-C. Structure and characterization of Sn, Al co-doped zinc oxide thin films prepared by sol-gel dip-coating process. *Thin Solid Films*. 2014;570: 516–526. doi:10.1016/j.tsf.2014.04.051
- [70] Dhruvashi, Shishodia PK. Effect of cobalt doping on ZnO thin films deposited by sol-gel method. *Thin Solid Films*. 2016;612: 55–60. doi:10.1016/j.tsf.2016.05.028
- [71] Wang LW, Wu F, Tian DX, Li WJ, Fang L, Kong CY, Zhou M. Effects of Na content on structural and optical properties of Na-doped ZnO thin films prepared by sol-gel method. *Journal of Alloys and Compounds*. 2015;623: 367–373. doi:10.1016/j.jallcom.2014.11.055
- [72] Jeng J-S. The influence of pH value and annealing temperature on the characteristics of ZnO–Ru composite films and their application in thin film transistors. *Microelectronic Engineering*. 2016;149: 1–4. doi:10.1016/j.mee.2015.08.014
- [73] Zhao J, Xie C, Yang L, Zhang S, Zhang G, Cai Z. Enhanced gas sensing performance of Li-doped ZnO nanoparticle film by the synergistic effect of oxygen interstitials and oxygen vacancies. *Applied Surface Science*. 2015;330: 126–133. doi:10.1016/j.apsusc.2014.12.194
- [74] Zhang XL, Hui KS, Bin F, Hui KN, Li L, Cho YR, Mane RS, Zhou W. Effect of thermal annealing on the structural, electrical and optical properties of Al–Ni co-doped ZnO thin films prepared using a sol-gel method. *Surface and Coatings Technology*. 2015;261: 149–155. doi:10.1016/j.surfcoat.2014.11.043
- [75] Peng S, Tang Y, Jin L, Wang Y, Ma L, Cao F. Comparison of the electro-optical performance of ZnO:Al and ZnO:B thin films derived by sol-gel method. *Surface and Coatings Technology*. 2017;310: 251–255. doi:10.1016/j.surfcoat.2016.12.090
- [76] Liu X, Pan K, Li W, Hu D, Liu S, Wang Y. Optical and gas sensing properties of Al-doped ZnO transparent conducting films prepared by sol-gel method under different heat treatments. *Ceramics International*. 2014;40: 9931–9939. doi:10.1016/j.ceramint.2014.02.090
- [77] Kafle BP, Acharya S, Thapa S, Poudel S. Structural and optical properties of Fe-doped ZnO transparent thin films. *Ceramics International*. 2016;42: 1133–1139. doi:10.1016/j.ceramint.2015.09.042
- [78] Pati S, Banerji P, Majumder SB. n- to p- type carrier reversal in nanocrystalline indium doped ZnO thin film gas sensors. *International Journal of Hydrogen Energy*. 2014;39: 15134–15141. doi:10.1016/j.ijhydene.2014.07.075
- [79] Xin M, Hu LZ, Liu D-P, Yu N-S. Effect of Mn doping on the optical, structural and photoluminescence properties of nanostructured ZnO thin film synthesized by sol-gel technique. *Superlattices and Microstructures*. 2014;74: 234–241. doi:10.1016/j.spmi.2014.06.009
- [80] Shewale PS, Patil VB, Shin SW, Kim JH, Uplane MD. H₂S gas sensing properties of nanocrystalline Cu-doped ZnO thin films prepared by advanced spray pyrolysis. *Sensors and Actuators B: Chemical*. 2013;186: 226–234. doi:10.1016/j.snb.2013.05.073

- [81] Hou Y, Jayatissa AH. Low resistive gallium doped nanocrystalline zinc oxide for gas sensor application via sol-gel process. *Sensors and Actuators B: Chemical*. 2014;204: 310–318. doi:10.1016/j.snb.2014.07.082
- [82] Khan F, Baek S-H, Kim JH. Influence of Ag doping on structural, optical, and photoluminescence properties of nanostructured AZO films by sol-gel technique. *Journal of Alloys and Compounds*. 2014;584: 190–194. doi:10.1016/j.jallcom.2013.09.055
- [83] Eskandari F, Ranjbar M, Kameli P, Salamati H. Laser induced photoconductivity in sol-gel derived Al doped ZnO thin films. *Journal of Alloys and Compounds*. 2015;649: 35–45. doi:10.1016/j.jallcom.2015.07.093
- [84] Ariyakkani P, Suganya L, Sundaresan B. Investigation of the structural, optical and magnetic properties of Fe doped ZnO thin films coated on glass by sol-gel spin coating method. *Journal of Alloys and Compounds*. 2017;695: 3467–3475. doi:10.1016/j.jallcom.2016.12.011
- [85] Shinde SS, Bhosale CH, Rajpure KY. Photoelectrochemical properties of highly mobilized Li-doped ZnO thin films. *Journal of photochemistry and photobiology B, Biology*. 2013;120: 1–9. doi:10.1016/j.jphotobiol.2013.01.003
- [86] Yilmaz M, Aydoğan S. The effect of Pb doping on the characteristic properties of spin coated ZnO thin films: Wrinkle structures. *Materials Science in Semiconductor Processing*. 2015;40: 162–170. doi:10.1016/j.mssp.2015.06.064
- [87] Davoodi A, Tajally M, Mirzaee O, Eshaghi A. Fabrication and characterization of optical and electrical properties of Al–Ti Co-doped ZnO nano-structured thin film. *Journal of Alloys and Compounds*. 2016;657: 296–301. doi:10.1016/j.jallcom.2015.10.107
- [88] Li B, Adjei R, Chen Z, Shen H, Luo J. Synthesis and characterization of highly preferred orientation polycrystalline Co-doped ZnO thin films prepared by improved sol-gel method. *Journal of Sol-Gel Science and Technology*. 2014;70: 19–23. doi:10.1007/s10971-014-3268-x
- [89] Amoupour E, Ghodsi FE, Andarva H, Abdolazadeh Ziabari A. Preparation and investigation of optical, structural, and morphological properties of nanostructured ZnO:Mn thin films. *Pramana*. 2013;81: 331–341. doi:10.1007/s12043-013-0566-8
- [90] Tsay C-Y, Hsu W-T. Sol-gel derived undoped and boron-doped ZnO semiconductor thin films: Preparation and characterization. *Ceramics International*. 2013;39: 7425–7432. doi:10.1016/j.ceramint.2013.02.086
- [91] Huang M-C, Lin J-C, Cheng S-H, Weng W-H. Influence of Ga dopant on photoelectrochemical characteristic of Ga-doped ZnO thin films deposited by sol-gel spin-coating technique. *Surface and Interface Analysis*. 2016. doi:10.1002/sia.6176
- [92] Senthil T, Anandhan S. Structure-property relationship of sol-gel electrospun ZnO nanofibers developed for ammonia gas sensing. *Journal of colloid and interface science*. 2014;432: 285–296. doi:10.1016/j.jcis.2014.06.029

- [93] Hou Y, Jayatissa AH. Effect of laser irradiation on gas sensing properties of sol-gel derived nanocrystalline Al-doped ZnO thin films. *Thin Solid Films*. 2014;562: 585–591. doi:10.1016/j.tsf.2014.03.089
- [94] Hou Y, Soleimanpour AM, Jayatissa AH. Low resistive aluminum doped nanocrystalline zinc oxide for reducing gas sensor application via sol-gel process. *Sensors and Actuators B: Chemical*. 2013;177: 761–769. doi:10.1016/j.snb.2012.11.085
- [95] Surendar T, Kumar S, Shanker V. Influence of La-doping on phase transformation and photocatalytic properties of ZnTiO₃ nanoparticles synthesized via modified sol-gel method. *Physical chemistry chemical physics : PCCP*. 2014;16: 728–735. doi:10.1039/c3cp53855a
- [96] Habibi MH, Sheibani R. Nanostructure silver-doped zinc oxide films coating on glass prepared by sol-gel and photochemical deposition process: Application for removal of mercaptan. *Journal of Industrial and Engineering Chemistry*. 2013;19: 161–165. doi:10.1016/j.jiec.2012.07.019
- [97] Thongsuriwong K, Amornpitoksuk P, Suwanboon S. Photocatalytic and antibacterial activities of Ag-doped ZnO thin films prepared by a sol-gel dip-coating method. *Journal of Sol-Gel Science and Technology*. 2012;62: 304–312. doi:10.1007/s10971-012-2725-7
- [98] Georgakopoulos T, Todorova N, Pomoni K, Trapalis C. On the transient photoconductivity behavior of sol-gel TiO₂/ZnO composite thin films. *Journal of Non-Crystalline Solids*. 2015;410: 135–141. doi:10.1016/j.jnoncrysol.2014.11.034
- [99] Chen Y, Zhang C, Huang W, Yang C, Huang T, Situ Y, Huang H. Synthesis of porous ZnO/TiO₂ thin films with superhydrophilicity and photocatalytic activity via a template-free sol-gel method. *Surface and Coatings Technology*. 2014;258: 531–538. doi:10.1016/j.surfcoat.2014.08.042
- [100] Kant S, Kumar A. A comparative analysis of structural, optical and photocatalytic properties of ZnO and Ni doped ZnO nanospheres prepared by sol-gel method. *Advanced Materials Letters*. 2012;3: 350-354.
- [101] Davar F, Majedi A, Mirzaei A, French R. Green Synthesis of ZnO Nanoparticles and Its Application in the Degradation of Some Dyes. *Journal of the American Ceramic Society*. 2015;98: 1739–1746. doi:10.1111/jace.13467
- [102] Abutaha AI, Sarath Kumar SR, Alshareef HN. Crystal orientation dependent thermoelectric properties of highly oriented aluminum-doped zinc oxide thin films. *Applied Physics Letters*. 2013;102: 053507. doi:10.1063/1.4790644
- [103] Liang X. Thermoelectric transport properties of Fe-enriched ZnO with high-temperature nanostructure refinement. *ACS Applied Materials & Interfaces*. 2015;7: 7927–7937. doi:10.1021/am509050a

